Design of Broadband Low Noise Amplifier Based on HEMT Transistors in the X-Band

Mohammed Lahsaini [#1], Lahbib Zenkouar [#2], Seddik Bri [*3]

[#] Electronic and Communication Laboratory, Mohammadia School of Engineers
EMI, Mohammed V University, Avenue Ibnsina B.P. 765 Agdal, Rabat, Morocco.
[1] mohammed.lahsaini@gmail.com
[2] zenkouar@emi.ac.ma
[*] Materials and Instrumentation Group, High School of Technology ESTM,
Moulay Ismail University, Meknes, Morocco
[3] briseddik@gmail.com

Abstract— **In this paper, we have modeled a low noise amplifier LNA based on HEMT transistors of Alpha Industries®, adapted by band pass filters in the X-band. A detailed study of performance optimizations for stability and noise of the different adaptation circuits was established. This amplifier is two-stage circuit. It is unconditionally stable in the band [8-12] GHz with a gain greater than 22.48 dB, a noise figure less than 1.1 dB and reflection coefficients at the input and output (S_{11}, S_{22}) less than -20 dB and - 40 dB respectively. The amplifier designed can be integrated in radar systems, amateur radio and civil and military radiolocation systems.**

Keyword- LNA, Adaptation, T and PI Circuits, Filters, Stability, Noise, Gain

I. INTRODUCTION

The low noise amplifier is one of the basic functional blocks in communication systems. The main interest of the LNA to the input of the analog processing chain is to amplify the signal without adding significant noise so as to allow a better analog and digital processing of information by following the modules of the LNA [1, 2].

The general structure of LNA includes an active device characterized by its S-parameters and surrounded on both sides by impedance adaptation networks. Adaptation networks of these amplifiers, especially when they have to be realized on a broadband, have always been considered a difficult exercise, feared by the majority of electronics specialists. This point is however very important, because this adaptation derives the optimization of transmitters and receivers hence link optimization. From several lines of investigation have been considered, giving as many procedures to solve the problem. Currently, it is not possible to conclude on the effectiveness or precision of one or other of these methods and to keep only one. Recent studies show that not everything has been said about the broadband adaptation. It comes usually to determine the values of three or four passive elements, inductors or capacities [2-5].

The objective of this paper is to model a broadband low noise amplifier based on HEMT transistors in the X-band with adaptation circuits of input and output with a minimum number of elements (inductors and capacities) giving satisfactory results compared with other articles by presenting the intermediate steps of the modeling of the amplifier so that anyone reading it can understand the various steps that led to the realization of the final circuit. First, we carry out a theoretical study of the circuit to stabilize and adapt it. Then we present some results of the study of the circuit (S-parameters, stability, gain, noise figure).

II. THEORY

A. HEMT Transistors

The heterojunction field effect transistor (HEMT: High Electron Mobility Transistor) is a component which operates near the MESFET. The difference is that the HEMT uses a heterojunction, that is to say a junction between materials having different energy bands, so as to move the electrons constituting the drain-source current in a non-doped semiconductor, to reduce the transit time and thus increase the performance in frequency. The speed of electrons is in fact even greater than the doping of the semiconductor is small because the dispersion of ionized impurities is reduced [3, 4]. The sectional view of a HEMT AlGaAs / GaAs is represented in Fig.1, as well as the conduction band profile corresponding. On a semi-insulating substrate a layer of undoped AsGa is deposited. The small-gap material allows the formation of the electron gas in the vicinity of the interface (large gap / low gap) with the AlGaAs layer. The electron gas created is then more or less dense following the polarization of the gate voltage.
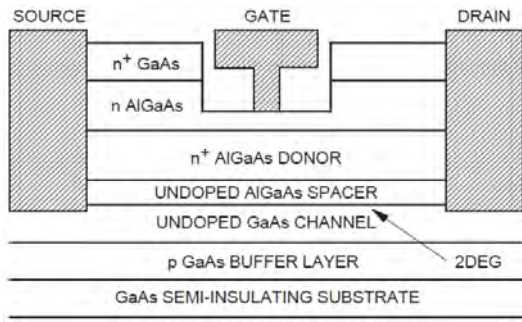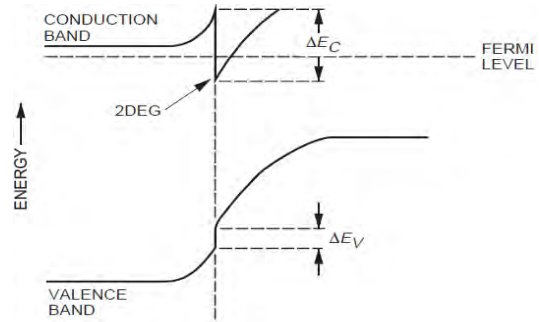
Fig. 1.   (a) Structure of a HEMT AlGaAs / GaAs   (b) Its conduction band diagram

The AlGaAs layer which provides electrons to the channel is highly doped on its upper part. Its lower part, called 'spacer', is itself undoped. This layer of a few tens of Angstroms improves the electron mobility by minimizing their interaction with the ionized donors. Finally, at the top of epitaxial structure of the HEMT a layer of heavily doped AsGa is deposited, which reduces the resistance of source and drain.

B. Adaptation

Generally, the power at the input of a system is determined by calculating the link budget. It is therefore important to maximize the gain of the amplifier stage in order to minimize the number of stages of the amplifier chain. This allows us to find the impedances $Z_1 = Z_{in}*$ and $Z_2 = Z_{out}*$ to present at the input and output of the transistor, in order to ensure the maximum transfer of power from the source to the load and the available power of the quadrupole [4-6].

There are different adaptation circuits among which we find the circuits in PI, T, and filters. In the following we present examples of calculations of these circuits.

1) Adaptation Circuits:

1-1) PI and T Circuits: The case of circuits in IP and T is an interesting case that allows to generalize the combination of adaptation networks. We can search the values of reactive elements L, C_1 and C_2 in Fig. 2, by giving the three equations of the system: adaptation and overvoltage coefficient of the loaded circuit. This leads to solving a relatively complex system. A simpler solution is to split the network in Fig. 2 into two simple L-networks, accordance with the scheme in Fig. 3 [5].
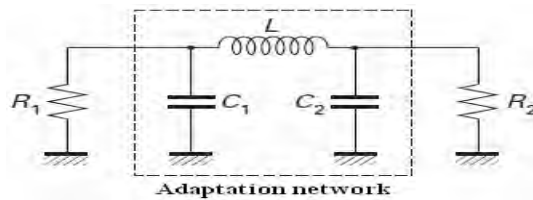

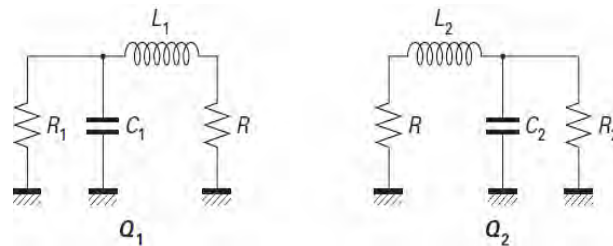Fig. 2. Adaptation between two real impedances R_1 and R_2 by a PI filter

Fig. 3. Transformation of PI filter of Fig. 2

1-2) PI Circuits: It concerns the processing of a set of two simple circuits, linked by a common value of the virtual intermediate resistance R. Each of these circuits has a loaded overvoltage coefficient Q_1 and Q_2.

The overvoltage coefficient of the circuit in PI, Q, is linked to Q_1 and Q_2 by the equation:

$$Q = Q_1 + Q_2 \qquad (1)$$

We can write the following equations:

- For the first network:

$$L_1 = \frac{R}{W}\sqrt{\frac{R_1 - R}{R}} = \frac{2Q_1 R}{W} \qquad \text{and} \qquad C_1 = \frac{1}{R_1 W}\sqrt{\frac{R_1 - R}{R}} = \frac{2Q_1}{W R_1} \qquad (2)$$

With $\quad Q_1 = \frac{1}{2}\sqrt{\frac{R_1 - R}{R}}$

– For the second network:

$$L_2 = \frac{R}{W}\sqrt{\frac{R_2 - R}{R}} = \frac{2Q_2 R}{W} \qquad \text{and} \qquad C_2 = \frac{1}{R_2 W}\sqrt{\frac{R_2 - R}{R}} = \frac{2Q_2}{WR_2} \qquad (3)$$

With $\quad Q_2 = \frac{1}{2}\sqrt{\frac{R_2 - R}{R}}$

The first step is to calculate the values of Q_1 and Q_2. In some works, this case is treated by imposing an arbitrary value for the value R. This can lead to an inaccurate result or approximate. Intermediate resistance R can simply be removed from the system of equations. It suffices to solve the system of equations [5].

$$Q = Q_1 + Q_2 \qquad (4)$$

$$Q_1 = \frac{1}{2}\sqrt{\frac{R_1 - R}{R}} \qquad (5)$$

$$Q_2 = \frac{1}{2}\sqrt{\frac{R_2 - R}{R}} \qquad (6)$$

For this system, there is only one solution simultaneously giving $Q_1 > 0$ and $Q_2 > 0$:

$$Q_1 = \frac{2QR_1 - \sqrt{2(1+2Q^2)R_1 R_2 - (R_1{}^2 + R_2{}^2)}}{2(R_1 - R_2)} \qquad (7)$$

$$Q_2 = \frac{-2QR_2 - \sqrt{2(1+2Q^2)R_1 R_2 - (R_1{}^2 + R_2{}^2)}}{2(R_1 - R_2)} \qquad (8)$$

This solution gives directly the result for the values of the two capacitors C_1 and C_2. The value of the inductor L is given by the relation:

$$L = L_1 + L_2 \qquad (9)$$

We put

$$A = \sqrt{2(1 + 2Q^2)R_1 R_2 - (R_1{}^2 + R_2{}^2)} \qquad (10)$$

The final result is then:

$$C_1 = \frac{2QR_1 - A}{(R_1 - R_2)R_1 W} \qquad \text{and} \qquad C_2 = \frac{-2QR_2 + A}{(R_1 - R_2)R_2 W} \qquad (11)$$

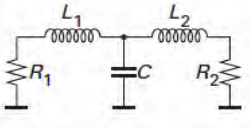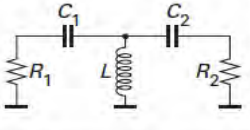$$L = L_1 + L_2 = \frac{2R}{W}Q \qquad (12)$$

Knowing that:

$$R = \frac{R_1}{1 + 4Q_1{}^2} \qquad (13)$$

$$L = \frac{2Q}{W}\frac{R_1}{1 + 4Q_1{}^2} = \frac{(R_1 - R_2)}{2W[Q(R_1 + R_2) - A]} \qquad (14)$$

1-3) T Circuits: The case of T circuits can be treated in a manner identical to the one used for the circuits in PI. The T network is split into two simple L networks, adapted to an intermediate resistance R of unknown value and the results are reported in Table I [4-5].

TABLE I
Adaptation between source and real load by T circuits

Circuit	L_1 ou C_1	L_2 ou C_2	L ou C
L_1 L_2 R_1 C R_2	$L_1 = \dfrac{R_1}{\omega}\dfrac{-2Q\,R_2 + A}{R_1 - R_2}$	$L_2 = \dfrac{R_2}{\omega}\dfrac{2Q\,R_1 - A}{R_1 - R_2}$	$C = \dfrac{2Q}{\omega R_1}\dfrac{(R_1 - R_2)^2}{(R_1 - R_2)^2 + (-2QR_2 + A)^2}$
C_1 C_2 R_1 L R_2	$C_1 = \dfrac{R_1 - R_2}{\omega R_1\,(-2QR_2 + A)}$	$C_2 = \dfrac{R_1 - R_2}{\omega R_2\,(-2QR_1 - A)}$	$L = \dfrac{2R_1 R_2}{\omega(R_1 - R_2)^2}\,[Q\,(R_1 + R_2) - A]$

2) Wideband Impedance Matching: When using a network including a capacitor and an inductor only, impedance matching is made perfectly on a particular frequency.

To consider an impedance matching over a wider bandwidth the number of cells should be multiplied. The network should be calculated to ensure that adaptation takes place exactly at two different frequencies [4-6].

2-1) Matching Network Low-Pass Type: Fig. 4 shows an impedance matching network includes four components: two inductors and two capacitors disposed between the resistances of source and load.
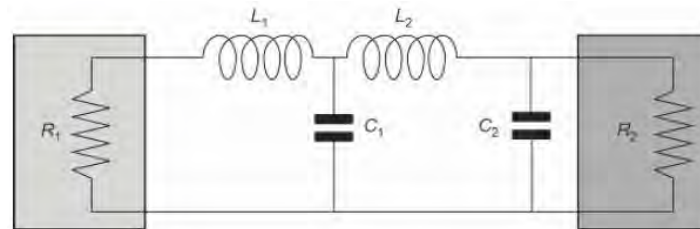

Fig. 4. Impedance matching by four components, low-pass type

To calculate the four components of this scheme, we must change its representation to display two complex impedances, one on the side of the source and the other on the side of the load. This new representation is given in Fig. 5 [5].

The complex impedances can be written:

- For the impedance seen towards the load:

$$Z_{ch} = \frac{R_2}{1 + R_2^2 C_2^2 W_2^2} + jw\left(L_2 - R_2\frac{R_2 C_2}{1 + R_2^2 C_2^2 W_2^2}\right) \tag{15}$$

- For the impedance seen towards the source:

$$Z_s = \frac{R_1}{R_1^2 C_1^2 W_1^2 + (L_1 C_1 W^2 - 1)^2} + jw\cdot\left(\frac{L_1(1 - L_1 C_1 W^2) - R_1^2 C_1}{R_1^2 C_1^2 W^2 + (L_1 C_1 W^2 - 1)^2}\right) \tag{16}$$
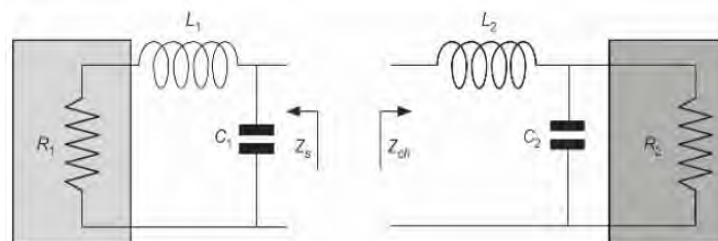

Fig. 5. Decomposition into real and imaginary part

To ensure that impedance matching can take place it is necessary that real parts are the same and that the imaginary parts are conjugated. These equalities must take place for two different frequencies f_1 and f_2 [2-5]. We are thus confronted with a system of four equations with four unknowns. The unknowns are the four values of the components L_1, L_2, C_1 and C_2.

The resolution of this system is not immediate, we must proceed carefully. By developing we obtain the following result:

$$L_1 = \frac{2}{AC_1} \qquad \text{and} \qquad L_2 = R_1 R_2 C_1 \tag{17}$$

$$C_1 = \frac{\sqrt{2}}{AR_1} \sqrt{A - B + \sqrt{B^2 - (\frac{A^2}{\alpha^2} - 2A(B - A))}} \quad \text{and} \quad C_2 = \frac{L_1}{R_1 R_2} \tag{18}$$

With $\quad A = 2\alpha w_1 w_2 \quad$ and $\quad B = W_1{}^2 + W_2{}^2$

This network can be used between two real impedances on condition that $R_2 > R_1$.

The capacitor C_2 can be dissociated into two parts, a part which becomes the complex part of the impedance on the side of R_2 and a part which remains on the side of the impedance matching circuit; Fig. 6 shows the changed adaptation network.
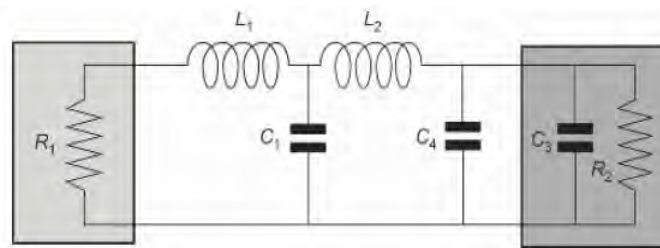

Fig. 6. Using of the matching network with a complex impedance

We can therefore do an adaptation between R_1 and R_2 - C_3, at first we ignore the capacitor C_3. At the end of the calculation the value of C_3 is subtracted from the value of C_2 calculated to obtain the value of the capacitor C_4 [4-5]:

$$C_2 = C_3 + C_4 \tag{19}$$

Note: In the case of adaptation networks for high-pass and band-pass, we adopt the same approach and the calculation of the four elements of the matching network is done by solving the system of equations for each of them.

C. Stability

1) Classical Criteria of Stability of Linear Microwave Circuit:

1-1) Rollett Coefficient K: The K factor, very widely used by designers to determine the stability of a linear quadrupole, is based on the determination of stability conditions according to the closing impedances presented in the access of the studied system.

A linear quadrupole, defined by its S distribution matrix is unconditionally stable if for any load impedance at positive real part placed at the input Z_S or at output Z_L, the module of the reflection coefficients at the input Γ_{in} and at the output Γ_{out} is less than 1 [1-4].

With:

$$\Gamma_{in} = S_{11} + \frac{S_{12} S_{21} \Gamma_L}{1 - S_{22} \Gamma_L} \qquad \text{and} \qquad \Gamma_{out} = S_{22} + \frac{S_{12} S_{21} \Gamma_S}{1 - S_{11} \Gamma_S} \tag{20}$$

This quadrupole is conditionally stable if one of two conditions is not verified for certain charges Z_S or Z_L, or for some pulsations w. Starting from relations $\Gamma_{in} < 1$ and $\Gamma_{out} < 1$, we obtain the stability criterion currently used.

$$\begin{cases} K = \frac{1 - |S_{11}|^2 - |S_{22}|^2 + |\Delta|^2}{2.|S_{12}|.|S_{21}|} \\ |\Delta| = |S_{11} S_{22} - S_{12} S_{21}| < 1 \end{cases} \tag{21}$$

Where Δ is the determinant of the S matrix of the quadrupole.
During the examination of the K factor, two cases may arise:
$K > 1$: Unconditional stability of the circuit regardless of the presented impedances.
$0 < K < 1$: Conditional stability of the circuit, some impedances can cause instability at certain frequencies.

1-2) Stability Coefficient μ: It should however be noted that the consideration of K factor doesn't allow to measure quantitatively the stability margin or degree of electrical instability of the studied device.

We are studying a criterion based on the same considerations as the previous [8], but more quantitative. This is the criterion μ introduced by M.L. Edwards and J.H. Sinsky [9]. This criterion allows to achieve the same conclusion with the criteria K> 1 and | Δ | <1 when μ> 1.

With:

$$\mu = \frac{1 - |S_{11}|^2}{|S_{22} - S_{11}^* \Delta| + |S_{12}S_{21}|} \tag{22}$$

In fact, μ is the minimum distance on the Smith chart between the origin (50 Ω) and the impedance of the closure nearest to the origin to cause instability.

If μ> 1: any point within the chart doesn't cause instability, so no passive load of circuit can cause instability.

If 0 <μ <1, in proportion as μ decreases, the number of stable closures on Smith chart is reduced.

If μ <0: the closure of 50 Ω causes instability, but we can find some impedances inside the unit circle which don't cause instability.

So, to know exactly the charges leading to instability, in the case where μ <1, we must draw circles of stability.

D. Noise Figure

The noise figure of a quadrupole characterizes the degradation of signal to noise ratio, between the input and the output of the quadrupole [6, 10], the generator being a dipole at the standard temperature T_0= 290 ° K:

$$F = \frac{\frac{P_e}{N_e}}{\frac{P_s}{N_s}} = \frac{P_{e_{disp}} \cdot N_{s_{disp}}}{P_{s_{disp}} \cdot N_{e_{disp}}} \tag{23}$$

F can be expressed with the available gain G_{disp}:

$$F = \frac{N_{s_{disp}}}{G_{disp} \cdot N_{e_{disp}}} \tag{24}$$

Consider the noisy quadrupole in Fig. 7. Attacked by a generator of noise voltage e_G and the impedance Z_G such as:

$$< e_G{}^2 > = 4.K.T_0.\Delta f.Re[Z_G] \tag{25}$$
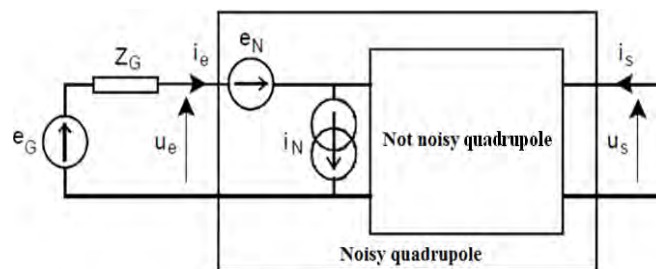
$$Z_G = R_G + jX_G \tag{26}$$

Fig. 7. Noisy quadrupole obedient to a noise voltage generator

If the sources of noise of the quadrupole reduced at the input having the same origin, they are correlated. We can define a correlation impedance Z_C as:

$$Z_c = R_c + jX_c \tag{27}$$

The correlation of the noise sources leads to:

$$e_N = e_{N_{nc}} - Z_c.i_N \tag{28}$$

With $e_{N_{nc}}$ the non-correlated part of noise voltage generator.

By developing we obtain:

$$F = 1 + \frac{r_N}{R_G} \cdot \frac{T}{T_0} + \frac{g_N}{R_G} \cdot \frac{T}{T_0} \, |Z_G + Z_c|^2 \tag{29}$$

- r_N: the equivalent resistance of noise of the quadrupole.

- g_N: the equivalent conductance of noise of the quadrupole.

The relation (29) shows that the noise figure of a quadrupole is a function of the impedance of the generator, or of the source if it's inserted in a circuit.

We can determine the optimum value of the impedance of the generator that makes the minimum noise figure [6].

By introducing the expressions of Z_G and Z_c, the noise figure is:

$$F = 1 + \frac{r_N}{R_G} + g_N \cdot \frac{(R_G + R_C)^2 + (X_G + X_C)^2}{R_G} \tag{30}$$

By developing we obtain:

$$F_{min} = 1 + 2.g_N \left(R_c + \sqrt{\frac{r_N}{g_N} + R_c{}^2} \right) \tag{31}$$

III. DESIGN OF LNA

A. Modeling of LNA in the X-Band

For modeling the low noise amplifier we have used the software simulation ADS (Agilent Device System) developed by Agilent®, this software is considered among the most powerful software at the level of design and simulation of electronic systems for microwave and radiofrequencies [11].

The structure of LNA modeled in Fig. 8 is composed of a bias stage, a stage of amplification and adaptation circuits in the form of band pass filters for the input and output. For the input, the filter composed of two L cells in cascade and for output in the form of a circuit in T.
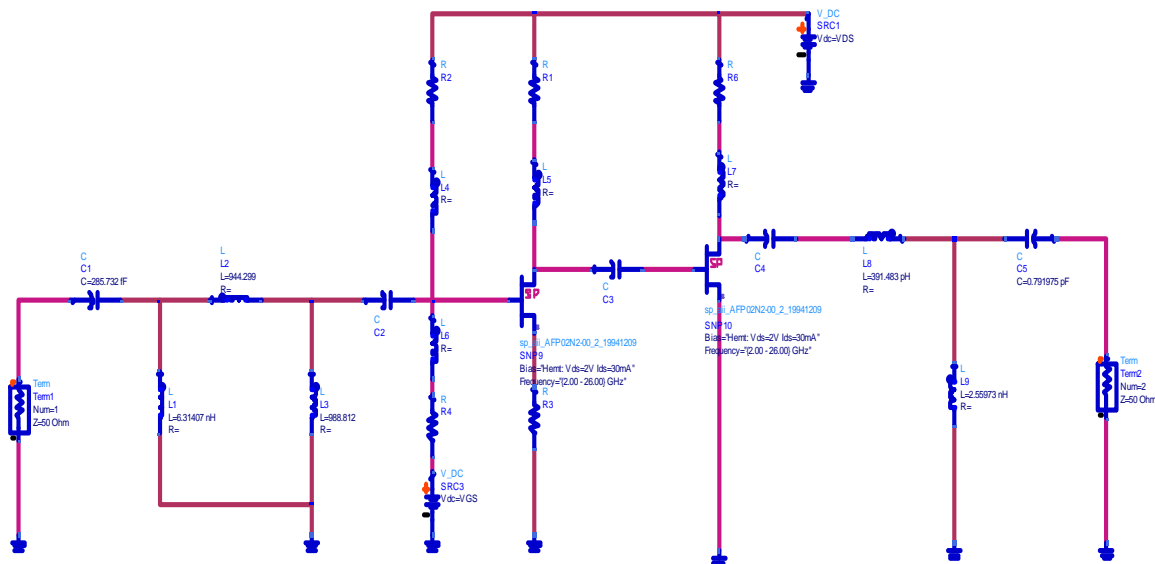

Fig. 8. General structure of the modeled amplifier

B. Results and Discussions

We have simulated the performance of circuit (Fig. 8) using optimization and adjustment techniques of ADS to determine the best values of components of the circuit giving a compromise between high gain and low noise value ensuring adaptation and stability of the amplifier. We obtained the following results:

The reflection coefficient S_{11} is strictly less than -20 dB and can reach the value -36.2 dB at 10.55 GHz (Fig. 9.a). S_{22} is less than -40 dB and can reach the value -73 dB at 9.55 GHz (Fig. 9.a).

For direct transmission coefficient S_{21} varies between 21.1 dB and 25.1 dB (Fig. 9.b). For the reverse transmission coefficient S_{12} varies between -36.6 dB and -41.4 dB (Fig. 9.b).
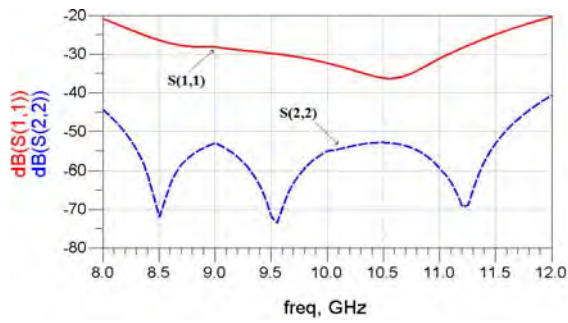
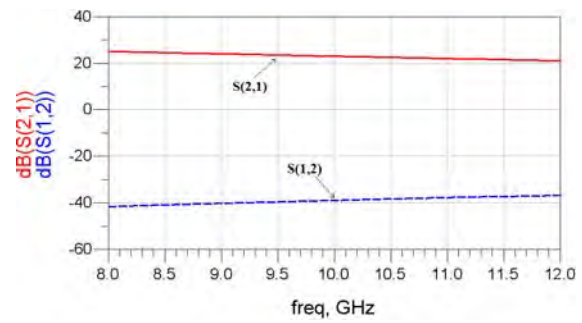Fig. 9.a Reflection coefficients (S_{11}, S_{22})   Fig. 9.b Transmission coefficients (S_{21}, S_{12})

For the stability of the LNA, the coefficients of stability at the input and at the output Mu1 and MuPrime1 are greater than 1 across the band of interest (Fig. 10.a), that is to say the LNA is unconditionally stable.

The noise of the LNA is less than 1.1 dB. The minimum noise figure NF_{min} varies from 0.65 to 0.97 dB (Fig. 10.b).
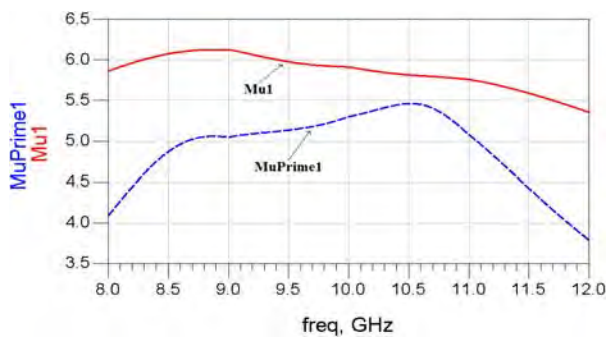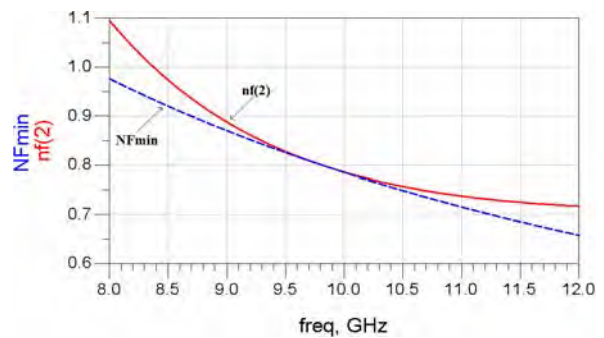

Fig. 10.a Stability coefficients   Fig. 10.b Noise of LNA

The voltage gain of LNA is greater than 22.48 dB across the X-band (Fig. 11).
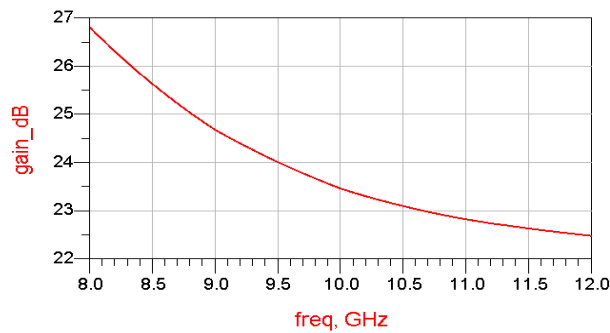

Fig. 11. Gain of LNA

Note: The voltage gain of LNA is expressed by the following equation:

$$G = 10 \log \left(\frac{V_s}{V_e}\right)^2 \text{ dB} \qquad (32)$$

With V_s and V_e are the input and output voltages of the circuit of (Fig. 8).

The Table II presents a summary of previously published results for different LNA based on emerging and promising technologies (HEMT, mHEMT, pHEMT and HBT) and compares them with this work. As shown in this table, the best performance of the amplifier results in low values of noise and S parameters (S_{11}, S_{22}, S_{12}), and high gain compared with other papers [12-15].

TABLE II
Comparison table of previously reported LNAs and this work

	BW (GHz)	S_{11} (dB)	S_{22} (dB)	S_{21} (dB)	S_{12} (dB)	Gain (dB)	NF (dB)	V_{DD} (V)	Technology
This work	**8 - 12**	**< -20**	**< -40**	**> 21**	**< -37**	**> 22.48**	**< 1.1**	**2**	**HEMT**
[12]	8 - 12	< -12	< -10.2	> 7.5	< -15	> 9.0	> 1.5	0.5	HEMT
[13]	8 - 12	< -4	< -2	> 22	*	> 12	< 1.4	1	mHEMT
[14]	8 - 12	< -15	< -0.4	> 7	*	18	< 2.4	2.4	HBT
[15]	8 - 12	< -8 .5	< -9.2	*	*	> 13	< 2.55	1.5	pHEMT

IV. CONCLUSION

In this paper an X-band low noise amplifier based on HEMT transistors was modeled, the LNA has a gain superior to 22.48 dB, a noise figure low enough less than 1.1 dB, an unconditional stability and a good adaptation from 8 to 12 GHz compared with other design techniques, the results demonstrate the excellent capacity of HEMT transistors and selected adaptation circuits. This amplifier can be integrated in radar systems, amateur radio and radiolocation civil and military systems.

REFERENCES

[1] Nelson, C. G. (2007). *High-Frequency And Microwave Circuit Design* (2nd edition ed.). (C. P. Group, Ed.)
[2] Pozar, D. M. (2005). *Microwave Engineering* (3 ed.). New York: John-Wiley & Sons.
[3] Razavi, B. (2011). *RF Microelectronics* (2nd edition ed.). (P. Hall, Ed.)
[4] Vendelin, G. D., Pavio, A. M., & Rohde, U. L. (2005). *Microwave circuit design using linear and nonlinear techniques* (2nd edition ed.). canada: John-Wiley & Sons.
[5] Françcois, d. D., & Olivier, R. (11 June, 2008). *Electronique Appliquée aux Hautes Fréquences: Principes et Applications* (2 ed.). Paris: Dunod.
[6] Villegas, M. C. (2008). Radio-Communications Numériques/2: Conception de Circuits Intégrés RF et Micro-ondes (2 ed.). Paris: Dunod.
[7] Tan, E. L., Sun, X., & An, K. S. (March 23-27,2009). Unconditional Stability Criteria for Microwave Networks. *PIERS Proceedings*, (pp. 1524-1528). Beijing, China.
[8] LOMBARDI, G., & NERI, B. (1999). Criteria for the evaluation of unconditional stability of microwave linear two-ports: a critical review and new proof. *IEEE Transactions on Microwave Theory and Techniques* , 47 (6), 746 - 751 .
[9] EDWARDS, M., & SINSKY, J. (1992). A new criterion for linear 2-port stability using a single geometrically derived parameter. *IEEE Transactions on Microwave Theory and Techniques* , 40 (12), 2303 - 2311.
[10] Haus, H. (2000). Noise figure definition valid from RF to optical frequencies. *IEEE Journal of Selected Topics in Quantum Electronics* , 6 (2), 240 - 247.
[11] Agilent Technologies. (2008, September). ADS, Design Guide Utilities.
[12] Liang, L., Alt, A., Benedickter, H., & Bolognesi, C. (2012). InP-HEMT X-band Low-Noise Amplifier With Ultralow 0.6-mW Power Consumption. *IEEE, Electron Device Letters* , 33 (2), 209 - 211 .
[13] Bhaumik, S., & Kettle, D. (2010). Broadband X-band low noise amplifier based on 70 nm GaAs metamorphic high electron mobility transistor technology for deep space and satellite communication networks and oscillation issues. *Microwaves, Antennas & Propagation, IET* , 4 (9), 1208 - 1215.
[14] Dogan, M., Div., E. -E., UEKAE, T. , Kocaeli, & Turkey Tekin, I. (25-27 Aug. 2010). A tunable X-band SiGe HBT single stage cascode LNA. *Microwave Symposium (MMS), 2010 Mediterranean*, (pp. 102 - 105).
[15] Mokerov, V., Gunter, V., Arzhanov, S., Fedorov, Y., Scherbakova, M., Babak, L., et al. (10-14 Sept. 2007). X-band MMIC Low-Noise Amplifier Based on 0.15 μm GaAs Phemt Technology. *Microwave & Telecommunication Technology, 2007. CriMiCo 2007. 17th International Crimean Conference*, (pp. 77 - 78). Moscow.